J Fluoresc (2015) 25:1323–1330
DOI 10.1007/s10895-015-1620-3

ORIGINAL ARTICLE

Design, Synthesis and Optoelectronic Properties of Unsymmetrical Oxadiazole Based Indene Substituted Derivatives as Deep Blue Fluoroscent Materials

Ningaraddi S. Belavagi[1] · Narahari Deshapande[1] · G. H. Pujar[2] · M. N. Wari[2] · S. R. Inamdar[2] · Imtiyaz Ahmed M. Khazi[1]

Received: 22 April 2015 / Accepted: 5 July 2015 / Published online: 22 July 2015

Abstract A series of novel unsymmetrically substituted indene-oxadiazole derivatives (**3a**–**f**) have been designed and synthesized by employing palladium catalysed Suzuki cross coupling reaction in high yields. The structural integrity of all the novel compounds was established by ^{1}H, ^{13}C NMR and LC/MS analysis. These compounds are amorphous in nature and are remarkably stable to long term storage under ambient conditions. The optoelectronic properties have been studied in detail using UV–Vis absorption and Fluorescence spectroscopy. All compounds emit intense blue to green-blue fluoroscence with high quantum yields. Time resolved measurments have shown life times in the range of 1.28 to 4.51 ns. The density functional theory (DFT) calculations were carried out for all the molecules to understand their structure–property relationships. Effect of concentration studies has been carried out in different concentrations for both absorption and emission properties and from this we have identified the optimized fluoroscence concentrations for all these compounds. The indene substituted anthracene-oxadiazole derivative (**3f**) showed significant red shift ($\lambda_{max}{}^{emi}$= 490 nm) and emits intense green-blue fluoroscence with largest stokes shift of 145 nm. This compound also exhibited highest fluoroscence life time (τ) of 4.51 ns, which is very close to the standard dye coumarin-540A (4.63 ns) and better than fluorescein-548 (4.10 ns). The results demonstrated that the novel unsymmetrical indene-substituted oxadiazole derivatives could play important role in organic optoelectronic applications, such as organic light-emitting diodes (OLEDs) or as models for investigating the fluorescent structure–property relationship of the indene-functionalized oxadiazole derivatives.

Keywords Amorphous materials · Chemical synthesis · Organic compounds · Optical properties · Computational technique

Introduction

Enormous development in the field of organic electronics [1] has enabled applications such as light-emitting diodes (LEDs), field-effect transistors (FETs), sensors and photovoltaics [2–5]. Extensive research has been carried out to promote organic light-emitting diodes (OLEDs) in commercial applications, such as flat-panel displays and solid-state lighting resources, due to their low cost [6–8]. OLEDs have been successfully utilized in mobile phones, computers, car stereos, digital cameras, wrist watches and white solid-state lighting [9–11]. The search for new and efficient emitting materials and charge transport layers remains one of the most active areas in this field [12, 13]. Since most of the organic compounds are inherently p-type (hole-transporting) semiconductors, considerable research has been focused on n-type (electron-transporting) materials for improved devices and complementary circuits [14–16]. One strategy for affecting n-type behavior is the inclusion of electron-withdrawing groups, especially 1,3,4-oxadiazole derivatives, which are one of the most widely studied class of electron-injection/

Electronic supplementary material The online version of this article (doi:10.1007/s10895-015-1620-3) contains supplementary material, which is available to authorized users.

✉ Imtiyaz Ahmed M. Khazi
drimkorgchem@gmail.com

[1] Department of Chemistry, Karnatak University, Dharwad 58003, Karnataka, India

[2] Department of Physics, Karnatak University, Dharwad 58003, Karnataka, India

hole-blocking materials due to their electron deficiency, high photoluminescence quantum yield, good thermal, and chemical stabilities. It has been shown previously that 2-(4-biphenylyl)-5-(4-tertbutylphenyl)-[1,3,4]-oxadiazole (PBD) functions very well as an excellent electron-transport material (ETM) in multilayer OLEDs [17].

Amorphous small organic molecules are good candidates for use in OLEDs [18–22] and also have other advantages over polymers and inorganic compounds like easy synthesis, purification and analysis. But the efficiency and life-time are the main limitations restricting the large scale, low cost manufacturing of multi-layered OLED devices. Incorporating unsymmetrical connection in small organic compounds prevents from crystallizing and yield higher thermal stability over that of symmetric derivatives [18, 23]. The development of the palladium-catalyzed cross-coupling Suzuki reaction of aryl halides with boronic acids provides an efficient and versatile means of extending π- π conjugation in organic compounds. In continuation of our research in the development of novel oxadiazoles for OLED applications [24, 25], herein we report a novel series of unsymmetrical indene substituted oxadiazoles, which shows intense blue-green fluoroscence can be explored for use in OLED applications.

In this study, we have designed and synthesized a series of novel unsymmetrical small organic molecules **3a**–**f** (Fig. 1) with indene substituted oxadiazole core moiety as an electron transporter, which are connected through a phenyl spacer with para linkages. The introduction of the indene moiety extends the π- π conjugation and oxadiazole moiety enhances the electron transporting capability because of the two withdrawing C=N groups, and also improves the thermal stability for better morphology. We have thoroughly investigated the optoelectronic properties like UV–Vis spectra, Fluorescence emitting spectra, Quantum yields, HOMO–LUMO calculations, Life-time measurements and Effect of concentration on the absorption/emission properties.

Experimental

Physical Measurements

All chemicals are reagent/analytical grade and used without further purification. Melting points were determined by open capillary method and are uncorrected. The IR spectra were recorded on Nicolet Impact 410 FT IR spectrophotometer using KBr pellets. ^{1}H and ^{13}C NMR were recorded on Bruker 400-MHz FT NMR spectrometer in $CDCl_3$ by using TMS as an internal standard. Chemical shifts are reported in ppm downfield (δ) from TMS. Mass spectra were recorded using Quadrupole LC/MS system with ESI resource. Elemental analysis were performed on a Vario III elemental analyzer. UV–Vis absorption spectra were recorded using JASCO UV–Vis NIR Spectrophotometer (Model V-670). Photoluminescence spectra were measured using Hitachi F-4500 fluorescence spectrophotometer. Fluorescence quantum yields (Φ) of the compound solutions were estimated by comparing wavelength-integrated photoluminescence (PL) intensity of the compound solutions with that of the reference. The lifetimes for the excited states were measured by employing picoseconds time domain spectrometer based on Time Correlated Single Photon Counting (TCSPC) technique (IBH Jobin Yvon6.1). The samples were excited at 375 nm using Nano LED in an IBH Fluorocube apparatus. The fluorescence emission at the magic angle was dispersed in a monochromatic (f/3) aperture and counted by a Hamamatsu Micro Channel Plate Photo-multiplier tube (R3809MCP-PMT). The instrument response function (IRF) for this system is ~373.12 ps. An iterative fitting program provided by IBH (DAS-6) analyzed the fluorescence decay curves.

Materials and Synthesis

The required intermediate 4-bromobenzhydrazide and OXD-bromides (**1a**–**f**) were synthesized according to the published

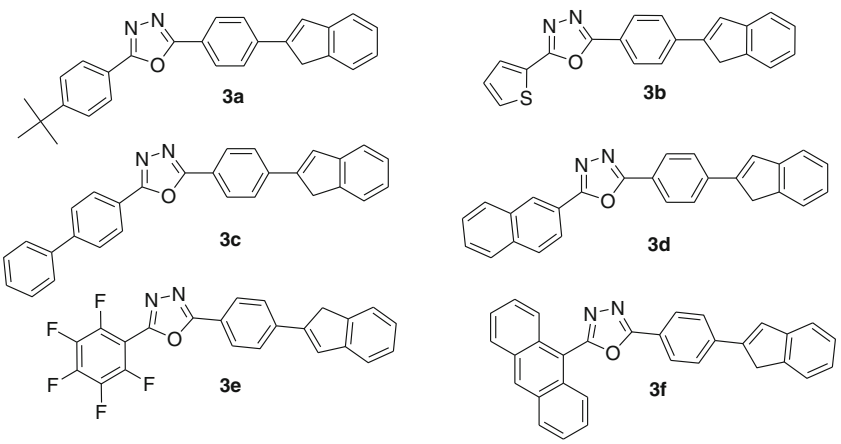

Fig. 1 Molecular structures of the designed indene-substituted oxadiazole derivatives **3a**–**f**

procedures [26]. The catalyst $Pd(dppf)_2Cl_2$ and 2-indenylboronic acid were purchased from commercial suppliers.

General Procedure for the Synthesis of Indene-Substituted Oxadiazole Derivatives (3a–f)

Under nitrogen atmosphere, OXD-bromides **1a**–**f** (0.5 g, 1.39 mmol), 2-indenylboronic acid (0.25 g, 1.54 mmol) and $Pd(dppf)Cl_2$ (0.051 g, 0.07 mmol) as a catalyst were added to a mixure of 1,4 dioxane (10 mL) and aqueous 2 M Na_2CO_3 (5 mL). The reaction was heated to 80 °C for 8 h. The progress of the reaction was monitored by TLC. The solvent was evaporated under reduced pressure. The residue was dissolved in DCM (25 mL), washed with H_2O (25 mL) and brine (25 mL). The organic phase was dried over anhydrous Na_2SO_4 and the solvent was evaporated, the residue was purified by column chromatography by eluting with Hexane/DCM (8:2, v/v). The title compounds were obtained as amorphous solids in 80–85 % yield.

2-(4-(1H-inden-2-yl)phenyl)-5-(4-tert-butylphenyl)-1,3,4-oxadiazole (3a) Yield: 82 %, Light ash colour. MP=240–242 °C. ^{1}H NMR (400 MHz, $CDCl_3$) δ: 8.07 (d, *J*= 8.4, 2H), 8.01 (d, *J*= 8.4 Hz, 2H), 7.71 (d, *J*= 8.4 Hz, 2H), 7.49 (d, *J*= 8.4, 2H), 7.44 (d, *J*= 7.2, 1H), 7.38 (d, *J*= 7.6, 1H), 7.30 (s, 1H), 7.23 (t, *J*= 7.4 Hz, 1H), 7.18 (d, *J*=7.4 Hz, 1H), 3.76 (s, 2H), 1.30 (s, 9H); ^{13}C NMR (100 MHz, $CDCl_3$) δ: 164.61, 164.27, 155.36, 145.03, 144.92, 143.32, 139.10, 128.83, 127.25, 126.84, 126.81, 126.06, 125.48, 123.81, 122.59, 121.49, 121.16, 38.91, 35.12, 31.15.; LC-MS (ESI): *m/z* calculated for $C_{27}H_{24}N_2O$ [M+H] 393.19, found 393.3; Anal. Calcd (%) for $C_{27}H_{24}N_2O$: C 82.62, H 6.16, N 7.14. Found: C 82.41, H 6.13, N 7.11

2-(4-(1H-inden-2-yl)phenyl)-5-(thiophen-2-yl)-1,3,4-oxadiazole (3b) Yield: 85 %, Brown colour. MP=210–212 °C. ^{1}H NMR (400 MHz, $CDCl_3$) δ: 8.05 (d, *J*= 8.0 Hz, 2H), 7.78 (d, *J*= 3.2 Hz, 1H), 7.70 (d, *J*= 8.4 Hz, 2H), 7.51 (d, *J*= 4.8, 1H), 7.44 (d, *J*= 7.2 Hz, 1H), 7..38 (d, *J*= 7.2 Mz, 1H), 7.31 (s, 1H), 7.23 (t, *J*= 7.4 Hz, 1H), 7.13 (t, *J*= 7.4 Hz, 1H), 3.76 (s, 2H); ^{13}C NMR (100 MHz, $CDCl_3$) δ: 162.80, 159.65, 143.83, 143.76, 142.20, 138.08, 129.11, 128.63, 127.80, 127.07, 126.15, 125.72, 124.93, 124.39, 124.19, 122.69, 121.07, 120.39, 37.77.; LC-MS (ESI): *m/z* calculated for $C_{21}H_{14}N_2OS$ [M+H] 343.08, found 343.2; Anal. Calcd (%) for $C_{21}H_{14}N_2OS$: C 73.66, H 4.12, N 8.18. Found: C 73.41, H 4.09, N 8.11

2-(4-(1H-inden-2-yl)phenyl)-5-biphenyl-1,3,4-oxadiazole (3c) Yield: 78 %, Light brown colour. MP=243–245 °C. ^{1}H NMR (400 MHz, $CDCl_3$) δ: 8.17 (d, *J*= 7.6 Hz, 2H), 8.11 (d, *J*= 8.0 Hz, 2H), 7.72 (t, *J*= 7.0 Hz, 4H), 7.61 (d, *J*= 8.0, 2H), 7.45–7.33 (m, 6H), 7.25 (t, *J*= 7.4 Hz, 1H), 7.17 (t, *J*= 7.4 Hz, 1H), 3.78 (s, 2H); ^{13}C NMR (100 MHz, $CDCl_3$) δ: 164.52, 164.35, 145.05 143.21, 139.12, 136.09, 136.51 129.29, 129.01, 128.38, 128.01, 129.0, 127.85, 127.65, 127.25, 126.84, 126.81, 126.06, 125.39, 125.24, 123.56, 122.43, 121.51, 121.21, 38.41.; LC-MS (ESI): *m/z* calculated for $C_{29}H_{20}N_2O$ 412.16, found 412.9; Anal. Calcd (%) for $C_{29}H_{20}N_2O$: C 82.62, H 6.16, N 7.14. Found: C 82.41, H 6.13, N 7.11

2-(4-(1H-inden-2-yl)phenyl)-5-(naphthalen-2-yl)-1,3,4-oxadiazole (3d) Yield: 85 %, Color: Light brown. MP=248–250 °C. ^{1}H NMR (400 MHz, $CDCl_3$) δ: 8.57 (s, 1H), 8.15 (m, 3H), 7.94 (d, *J*= 8.4 Hz, 2H), 7.84 (s, 1H), 7.74 (d, *J*= 8.0, 2H), 7.53 (m, 2H), 7.45 (d, J=7.2 Hz, 1H), 7.39 (d, J=7.6 Hz, 1H), 7.33 (s, H), 7.24 (t, *J*= 7.4 Hz, 1H), 7.17 (t, *J*= 7.4 Hz, 1H), 3.78 (s, 2H); ^{13}C NMR (100 MHz, $CDCl_3$) δ: 164.52, 145.21, 143.15, 139.41, 136.79, 134.35, 133.78, 129.32, 129.12, 128.6, 128.11, 127.88, 127.37, 126.91, 126.29, 126.22, 125.78, 123.89 122.71, 121.85, 121.32, 38.95; LC-MS (ESI): *m/z* calculated for $C_{27}H_{18}N_2O$ [M+H] 387.14, Found 387.3; Anal. Calcd (%) for $C_{27}H_{18}N_2O$: C 83.92, H 4.69, N 7.25. Found: C 83.78, H 4.57, N 7.28

2-(4-(1H-inden-2-yl)phenyl)-5-(perfluorophenyl)-1,3,4-oxadiazole (3e) Yield: 75 %. Color: Off white. MP=233–235 °C. ^{1}H NMR (400 MHz, $CDCl_3$) δ: 8.07 (d, *J*= 8.4 Hz, 2H), 7.73 (d, *J*= 8.4 Hz, 2H), 7.45 (d, *J*= 7.2 Hz, 1H), 7.39 (d, *J*= 7.6 Hz, 1H), 7.34 (s, 1H), 7.24 (t, *J*= 7.4 Hz, 1H), 7.17 (d, *J*= 7.4 Hz, 1H) 3.77 (s, 2H); ^{13}C NMR (100 MHz, $CDCl_3$) δ: 165.68, 144.77, 143.34, 139.97, 129.39, 127.66, 126.91, 126.21, 125.68, 123.84, 121.61, 121.45, 38.91; ^{19}F NMR (400 MHz, $CDCl_3$) δ: −135.33, −147.23, −159.49; LC-MS (ESI): *m/z* calculated for $C_{23}H_{11}F_5N_2O$ [M+H] 427.08, found 427.0; Anal. Calcd (%) for $C_{23}H_{11}F_5N_2O$: C 64.80, H 2.60, N 6.57. Found: C 64.69, H 2.56, N 6.51

2-(4-(1H-inden-2-yl)phenyl)-5-(anthracen-10-yl)-1,3,4-oxadiazole (3f) Yield: 84 %. Color: Yeloow. MP=254–256 °C. ^{1}H NMR (400 MHz, $CDCl_3$) δ: 8.63 (s, 1H), 8.14 (d, *J*= 8.4 Hz, 2H), 8.03 (m, 4H), 7.74 (d, *J*= 8.4 Hz, 2H), 7.50 (m, 4H), 7.41 (m, 2H), 7.33 (s, 1H), 7.24 (t, *J*= 7.4, 1H), 7.16 (t, *J*= 7.4, 1H), 3.78 (s, 2H); ^{13}C NMR (100 MHz, $CDCl_3$) δ: 164.48, 145.11, 143.13, 139.39, 139.21, 136.81, 136.01, 130.22, 129.32, 129.10, 128.62, 128.25, 127.88, 127.37, 126.91, 126.29, 126.22, 125.78, 123.89 122.64, 121.715, 121.22, 39.13; LC-MS (ESI): *m/z* calculated for $C_{31}H_{20}N_2O$ [M+H] 437.16, found 437.2; Anal. Calcd (%) for $C_{31}H_{20}N_2O$: C 85.30, H 4.62, N 6.42. Found: C 85.42, H 4.33, N 6.51

Results and Discussion

Synthesis and Characterization

The molecular structures of target unsymmetrical indene-oxadiazole derivatives (**3a**–**f**) are illustrated in Fig. 1. Relatively simple and efficient synthetic protocols were used to synthesize the target compounds and the synthetic details are illustrated in Scheme 1. The 2-indenyl-phenyl substituent is kept constant in the second position of oxadiazole ring and in the fifth position we have incorporated different substituents such as p-tert-butylphenyl, thiophen-2-yl, biphenyl, 2-napthyl, pentafluorophenyl and anthracene to modify their spectral properties. The required starting material 4-bromobenzohydrazide was obtained from commercially available 4-bromobenzoic acid on esterification followed by treating with hydrazine hydrate as per the reported literature [27, 28]. The key intermediates OXD-bromides (**1a**–**f**) were synthesized by treatment of 4-bromobenzohydrazide with various aromatic carboxylic acids in refluxing $POCl_3$ [17, 24]. Subsequent Pd-catalyzed Suzuki cross-coupling reaction between the OXD-bromides (**1a**–**f**) and 2-Indenylboronic acid (**2**) afforded the unsymmetrical target compounds (**3a**–**f**) in 75–85 % yields. All compounds were purified by column chromatography on silica gel followed by recrystallization in ethanol before spectral characterization. All these compounds are amorphous in nature and are stable to routine purification and can be stored under ambient conditions for long term without any detectable decomposition. These compounds are readily soluble in common organic solvents like EtOH, $CHCl_3$, DCM and THF etc. Their structural identities and purities were confirmed by ^{1}H NMR, ^{13}C NMR, IR and LC/MS and elemental analysis (see Supporting information).

UV–Vis Absorption and Fluoroscence Spectra

Figure 2 shows the UV–Vis absorption spectra of compounds **3a**–**f** in ethanol (HPLC grade) at room temperature and the corresponding photo-physical data are listed in Table 1. The electronic absorption spectra of all compounds have similar absorption peaks in the range from 341 to 355 nm and these characteristic bands are assigned to the π-π* transitions of the extended conjugative indene-OXD-aryl chain. Additionally, strong absorption bands at the high energy 200–220 nm region, corresponding to the spin-allowed, π-π* transitions, the so-called K band absorption of the indene group. In the series, the biphenyl derivative **3c** showed least λ_{max}^{abs} of 341 nm and the 2-naphtyl derivative **3d** exhibited highest λ_{max}^{abs} of 355 nm.

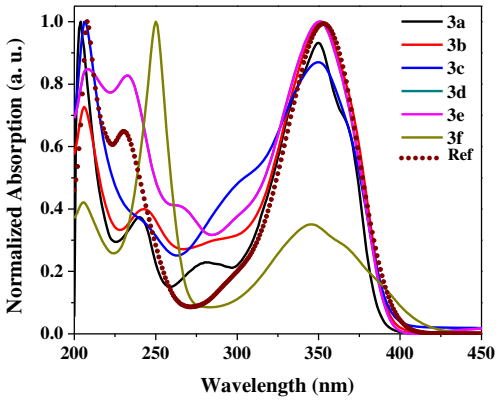

Fig. 2 Normalized UV–Vis absorption spectra of compounds **3a**–**f** in ethanol at room temperature (Optical Density concentration 0.1 a.u.) compared with Reference (Coumarin 440)

Figure 3 shows the real scale photoluminescence (PL) spectra, which could provide a good deal of information on the electronic structure of the conjugated compounds, as oxadiazole itself is an electron deficient system having three electron rich atoms delocalized over the ring that can act as a π-electron acceptor; incorporation of electron rich indene and aryl groups at the 2nd and 5th position of oxadiazole ring alters the maximum emission and intensity which in turn affects the quantum yield of the compounds. This implies interaction of the electron rich bulky groups at 2nd and 5th positions of oxadiazole backbone and internal charge transfer along the oxadiazole backbone in the excited state to enhance

Scheme 1 Reaction scheme for the synthesis of key intermediates (**1a**–**f**) and target compounds (**3a**–**f**)

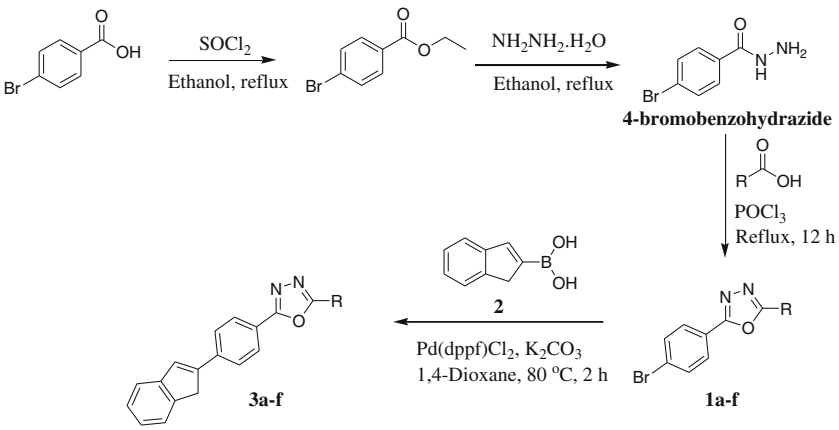

Table 1 Photo physical & Time resolved measurements of compounds **3a-f**

Compounds	Absorption λ_{max}^{abs} (nm)[a]	Emission λ_{max}^{emi} (nm)[a]	Stokes shift $\Delta\lambda$ (nm)	Quantum Yield	Life Time τ (ns)	Optimized Fluoroscence Concentration *(μM)*
3a	349	410	61	0.45	1.286	8
3b	351	423	72	0.40	1.332	80
3c	341	416	75	0.40	1.305	10
3d	355	416	61	0.51	1.378	20
3e	349	421	72	0.27	1.653	4
3f	345	490	145	0.26	4.514	4
Ref[b]	351	427	76	0.98	*nd*	nd
Ref[c]	nd	nd	nd	nd	4.63	nd
Ref[d]	nd	nd	nd	nd	4.10	nd

nd not determined

[a] The absorption and emission spectra were measured in ethanol at room temperature (Optical Density concentration 0.1 a.u.)

[b] Coumarin 440

[c] Coumarin 540A

[d] Fluorescein 548

luminescence intensity. The least overlapping of the emission and absorption spectra of these compounds indicate that reabsorption of the emitted light by the compounds is negligible. The PL spectra of all these compounds (**3a–f)** in ethanol at room temperature were found to exhibit excellent blue emission with the peak maxima λ_{max}^{emi} in the range of 410 to 490 nm. The anthracene derivative **3f** displayed a significant red-shifted PL emission with a broad λ_{max}^{emi} at 490 nm (emits blue-green light) compared to other compounds in the series. This is due to the bulky anthracene group, which makes the compound **3f** to have extended conjugation length and the degree of intermolecular interaction could lead to the formation of excimers or aggregates.

The stokes shift, indicating the extent of the red shift of the fluorescence maxima (λ_{max}^{emi}) compared to the absorption maxima (λ_{max}^{abs}) is in the range of 61–145 nm. The lowest stokes shift for compounds **3a** and **3d** is 61 nm and is higher for **3c** (75 nm) and it is highest for **3f** (145 nm) indicating the more structural changes between the ground and excited state of **3f** compared to other compounds in the series and is therefore connected with the difference in the intramolecular charge transfer (ICT) character of the ground state of these molecules.

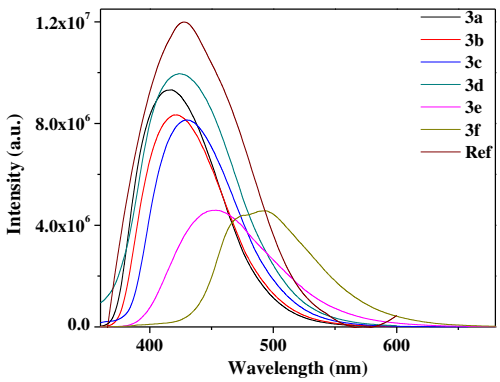

Fig. 3 PL spectra of compounds **3a-f** in ethanol at room temperature (Optical Density concentration 0.1 a.u.) compared with Reference (Coumarin 440)

Computational Methods

To have a deeper understanding on the structure–property relationship, we performed theoretical calculations on the frontier molecular orbitals via DFT/B3LYP/6-31G method using the Guassian 09 program [29] for the geometry optimization. The ground state optimized molecular structures and frontier molecular orbitals for all compounds shown in Fig. 4. The Highest Occupied Molecular Orbitals (HOMO) and Lowest Unoccupied Molecular Orbitals (LUMO) and their energy band gap (E_g) values are tabulated in Table 2. It is interesting to note that the HOMOs of all compounds are mostly localized on the electron donating indene-phenyl center, whereas the LUMOs are shifted to the peripheral electron accepting oxadiazole moieties, leading to an obvious spatial separation of frontier orbitals. In contrast, the HOMO and LUMO of anthracene derivative **3f** are effectively delocalized over the electron donating and accepting moieties, leading to a weak trend of charge transfer upon photo excitation. The computationally calculated HOMO and LUMO energy values are in the range of −5.39 to −5.78 eV and 1.99–2.64 eV, respectively. Small variations in HOMO and LUMO energy values for all compounds indicate a similar electronic

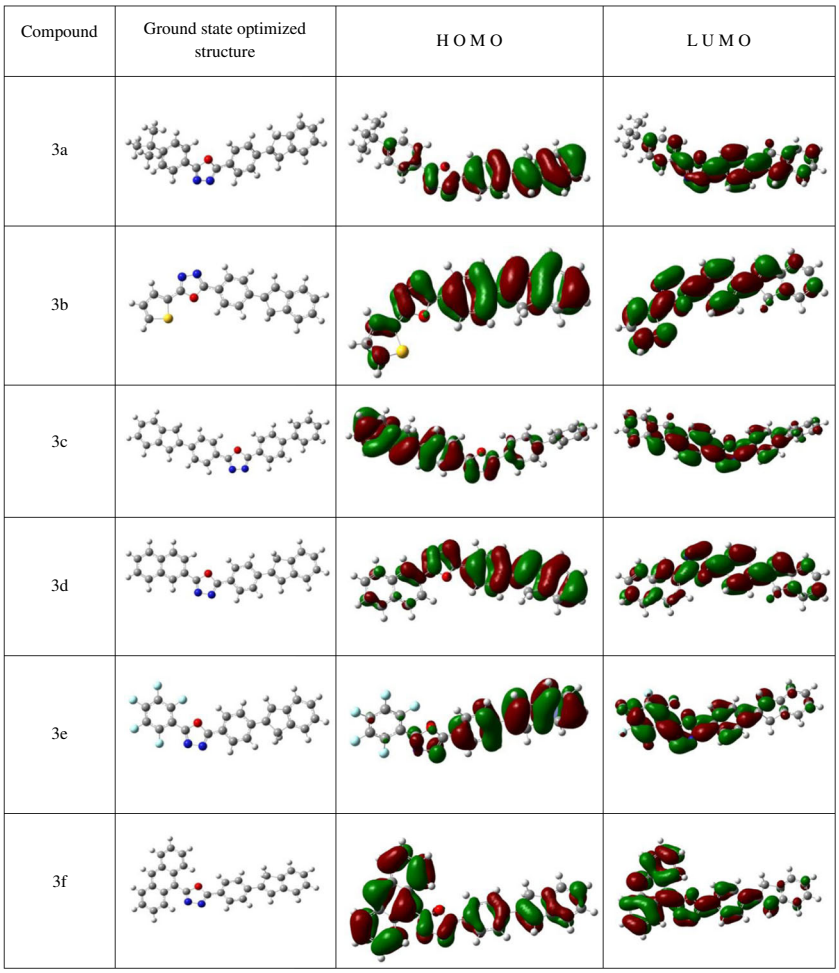

Fig. 4 Ground state optimized structures and Frontier molecular orbitals (HOMO and LUMO) of **3a–f** calculated by the DFT/B3LYP/6-31G method

structure. Optical band gaps obtained from absorption spectrum are in the range of 3.49–3.64 eV which is in good agreement with the band gaps (3.14–3.54 eV) obtained using DFT method.

Table 2 Optical band gap obtained from DFT and UV–Vis absorption spectrum for comparison

Compounds	HOMO (eV)[a]	LUMO (eV)[a]	ΔE (eV)[a]	ΔE_{opt} (eV)[b]
3a	−5.53838	−1.99869	3.54	3.20 (388)
3b	−5.56532	−2.15924	3.41	3.15 (394)
3c	−5.55334	−2.07597	3.48	3.15 (393)
3d	−5.54681	−2.07244	3.47	3.15 (394)
3e	−5.78247	−2.64089	3.14	3.15 (393)
3f	−5.39769	−2.22346	3.17	3.00 (413)

where λ is the edge wavelength (in nm) of the UV–Vis absorption spectrum

[a] Obtained using DFT/B3LYP/6-31G method, ΔE=HOMO−LUMO (eV)

[b] Optical band gap energies were calculated from the equation E_{opt}=hc/λ=1240/λ (eV)

Quantum Yield (Φ) and Life Time Measurements (τ)

Fluorescence quantum yields (Φ) of the all the compounds were measured in ethanol at room temperature by comparison with a standard dye Coumarin 440 (C120) of known quantum yield (Φ=0.98) [27, 30] using the Eq. 1.

$$\Phi = \Phi_R \frac{I}{I_R} \frac{OD_R}{OD} \frac{n^2}{n_R^2} \quad (1)$$

Where I is the integrated intensity, OD is the optical density and n is the refractive index, the subscript R refers to the reference fluorophore of known quantum yield. The quantum yields of all the compounds are in the range of 0.26 to 0.51 (Table 1). The 2-napthyl derivative **3d** exhibited higher quantum yield of 0.5 and substantial decrease in the quantum yield for the anthracene derivative (**3f**) to be 0.26 because of low emission intensity which is attributed to the photoinduced intramolecular charge transfer (ICT) processes [31, 32]. The decrease in quantum yield resulting from the photoinduced ICT process is a common phenomenon for organic compounds [33, 34].

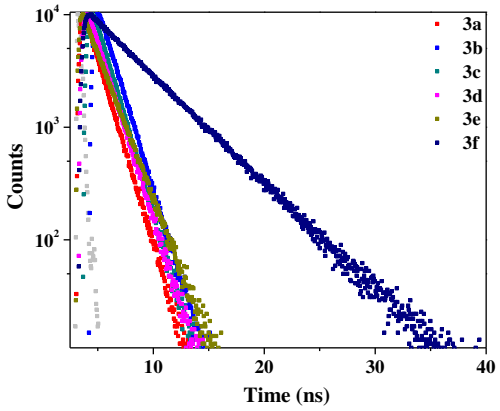

Fig. 5 Log scale plot of time-resolved PL traces of **3a–f**

Figure 5 shows the experimentally determined fluorescence lifetimes (τ) for all compounds and is in the range of 1.28–4.51 ns. The p-tert-butylphenyl derivative **3a** has shown the least life time of 1.28 ns, an anthracene derivative **3f** showed highest life time of 4.51 ns and the remaining compounds have shown life times between 1.30 and 1.65 ns. The life time of anthracene derivative **3f** (4.51 ns) is very close to the standard dye Coumarin-540A (4.63 ns) and is better than Fluorescein-548 (4.10 ns) indicating the good lasing property.

Effect of Concentration on the Absorption/Emission Properties

To evaluate the effect of concentration on absorption-emission properties of all the synthesized compounds **3a–f**, we have recorded the absorption and emission spectra in different concentrations for all compounds. In the absorption spectra, the intensity of absorption gradually increased with increasing concentrations from 0.05 μM to 10 μM which is an ideal condition for good OLED compounds. The representative absorption spectrum of **3f**, which shows the effect of concentration is shown in Fig. 6. In the emission spectrum of all the compounds, initially the intensity of emission gradually increased with increasing concentration and reached a maximum (optimized concentration) and then gradually decreased due to self quenching. We have identified the optimized fluoroscence concentration for all the synthesized compounds and are summarized in Table 1 and representative PL spectrum of **3f**, which shows the effect of concentration on the intensity of emission is shown in Fig. 7. The thiophene derivative (**3b**) has the highest optimized fluoroscence concentration of 80 μM and the pentafluorophenyl derivative (**3e**) has the lowest optimized fluoroscence concentration of 4 μM.

Conclusion

In summary, we have successfully synthesized a series of novel unsymmetrical indene-substituted oxadiazole derivatives as blue emitters for use in organic light emitting diodes (OLEDs) by employing palladium catalysed Suzuki cross coupling reactions in high yields. The synthesized compounds were confirmed by FT-IR, ^{1}H NMR, ^{13}C NMR and Mass spectral analysis. All these compounds are amorphous in nature and are remarkably stable to long term storage under ambient conditions. The photo physical properties have been studied in detail using UV–Vis absorption and fluorescence spectroscopy. All compounds emit intense blue to green-blue fluoroscence with good quantum yields. The fluorescence quantum yield was found to be excellent (0.51) for 2-napthyl derivative (**3d**). Computationally we have calculated HOMO-LUMO energy values for all compounds using DFT method and their small band gap energy values indicate similar electronic structure. Optical band gaps obtained from absorption spectrum are in good agreement with the band gaps obtained from DFT method. We have evaluated the effect of concentration on the absorption and emission spectra of all the synthesized compounds. With increasing concentration the intensity of absorption gradually increases where as the intensity of emission initially increases and reaches a maximum (Optimized fluoroscence concentration) and then decreases at higher concentration due to self-absorption. We have identified the

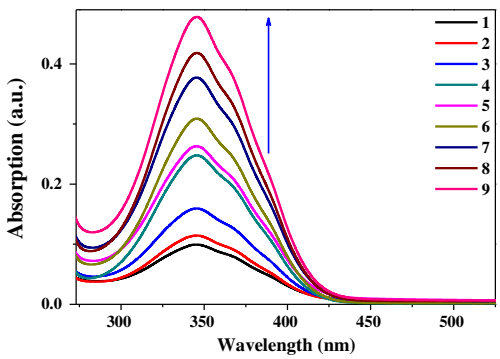

Fig. 6 Effect of concentration on the absorption spectra of **3f** in ethanol; (*1*) 0.5 μM, (*2*) 1 μM, (*3*) 2 μM, (*4*) 4 μM, (*5*) 6 μM, (*6*) 8 μM, (*7*) 10 μM, (*8*) 20 μM, (*9*) 40 μM. λ_{max}^{abs}=349 nm

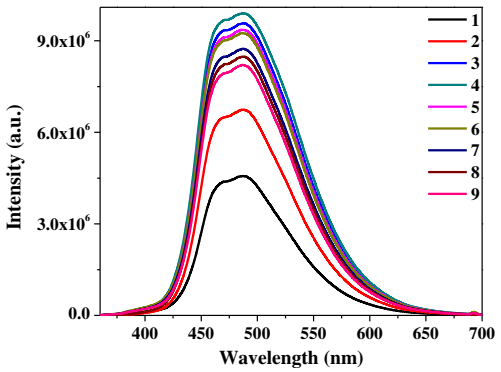

Fig. 7 Effect of concentration on the emission spectra of **3f** in ethanol; (*1*) 0.5 μM, (*2*) 1 μM, (*3*) 2 μM, (*4*) 4 μM, (*5*) 6 μM, (*6*) 8 μM, (*7*) 10 μM, (*8*) 20 μM, (*9*) 40 μM. λ_{max}^{abs}=349 nm

optimized fluoroscence concentration for all the compounds. Time resolved measurements have shown lifetimes in the range 1.28–4.51 ns. Among the compounds, anthracene derivative (**3f**) showed a significant red shift (λ_{max}^{emi}=490 nm) and emits intense green-blue fluoroscence with largest stokes shift of 145 nm. This compound also exhibited highest fluoroscence lifetime (τ) of 4.51 ns, which is very close to the standard dye Coumarin-540A (4.63 ns) and is better than Fluorescein-548 (4.10 ns) indicating good lasing property. The results demonstrated here indicate that the new unsymmetrical indene-substituted oxadiazole derivatives could play important role in organic optoelectronic applications, such as organic light-emitting devices (OLEDs) or as models for investigating the fluorescent structure–property relationship of the indene-functionalized oxadiazole derivatives.

Acknowledgments We are thankful for the financial assistance from UGC, New Delhi under CPEPA and UPE-FAR-I programmes. NSB is thankful for the Research Fellowship under UPE FAR-I (F. No. 14-3/2012 (NS/PE), ND & GHP are thankful for the Research Fellowship under CPEPA (No. 8-2/2008(NS/PE). We greatly acknowledge University Science Instrumentation Centre for spectral analysis.

References

1. Tannaci JF, Noji M, McBee JL, Tilley TD (2008) J Org Chem 73: 7895
2. Kulkarni AP, Tonzola CJ, Babel A, Jenekhe SA (2004) Chem Mater 16:4556
3. Zaumseil J, Sirringhaus H (2007) Chem Rev 107:1296
4. Thomas SW, Joly GD, Swager TM (2007) Chem Rev 107:1339
5. Thompson BC, Fre'chet JMJ (2008) Angew Chem Int Ed 47:58
6. Mallesham G, Balaiah S, Ananth Reddy M, Sridhar B, Singh P, Srivastava R, Bhanuprakash K, Rao VJ (2014) Photochem Photobiol Sci 13:342
7. Zhu M, Yang C (2013) Chem Soc Rev 42:4963
8. Yoo S, Yun H, Kang I, Thangaraju K, Kwon S, Kim Y (2013) J Mater Chem C 1:2217
9. Nuyken O, Jungermann S, Wiederhirn V, Bacher E, Meerholz K (2006) Monatsh Chem 137:811
10. Kim YH, Lee SJ, Jung SY, Byeon KN, Kim JS, Shin SC, Kwon SK (2007) Bull Kor Chem Soc 28:443
11. Adhikari RM, Mondal R, Shah BK, Neckers DC (2007) J Org Chem 72:4727
12. Xu X, Yu G, Chen S, Di C, Liu Y (2008) J Mater Chem 18:299
13. Tong Q, Lai S, Chan M, Zhou Y, Kwong H, Lee C, Lee S (2008) Chem Mater 20:6310
14. Strukelj M, Papadimitrakopoulos F, Miller TM, Rothberg LJ (1995) Science 267:1969
15. Yoo B, Jones BA, Basu D, Fine D, Jung T, Mohapatra S, Facchetti A, Dimmler K, Wasielewski MR, Marks TJ, Dodabalapur A (2007) Adv Mater 19:4028
16. Katz HE, Lovinger AJ, Johnson J, Kloc C, Siegrist T, Li W, Lin YY, Dodabalapur A (2000) Nature 404:478
17. Tao Y, Yang C, Qin J (2011) Chem Soc Rev 40:2943
18. Zhu CC, Guo KP, Liu WB, He YB, Li ZM, Gao XC, Deng FJ, Wei B (2013) Opt Mater 35:2095
19. Okumoto K, Shirota Y (2001) Mater Sci Eng B 85:135
20. Kageyama H, Ohishi H, Tanaka M, Ohmori Y, Shirota Y (2010) IEEE J Quantum Electron 16:1528
21. Promarak V, Ichikawa M, Sudyoadsuk T, Saengsuwan S, Jungsuttiwong S, Keawin T (2008) Thin Solid Films 516:2881
22. Shirota Y (2000) J Mater Chem 10:1
23. Koene BE, Loy DE, Thompson ME (1998) Chem Mater 10:2235
24. Panchamukhi SI, Belavagi N, Rabinal MH, Khazi IA (2011) J Fluoresc 21:1515
25. Deshapande N, Belavagi NS, Panchamukhi SI, Rabinal MH, Khazi IAM (2014) Opt Mater 37:516
26. Dawson WR, Windsor MW (1968) J Phys Chem 72:3251
27. Wang C, Pålsson L-O, Batsanov AS, Bryce MR (2006) J Am Chem Soc 128:3789
28. Shailaja M, Anitha M, Manjula A, Rao BV (2010) Indian J Chem 49B:1088
29. Frisch MJ, Trucks GW, Schlegel HB, Scuseria GE, Robb MA, Cheeseman JR, Scalmani G, Barone V, Mennucci B, Petersson GA, Nakatsuji H, Caricato M, Li X, Hratchian HP, Izmaylov AF, Bloino J, Zheng G, Sonnenberg JL, Hada M, Ehara M, Toyota K, Fukuda R, Hasegawa J, Ishida M, Nakajima T, Honda Y, Kitao O, Nakai H, Vreven T, Montgomery JA Jr, Peralta JE, Ogliaro F, Bearpark M, Heyd JJ, Brothers E, Kudin KN, Staroverov VN, Kobayashi R, Normand J, Raghavachari K, Rendell A, Burant JC, Iyengar SS, Tomasi J, Cossi M, Rega N, Millam JM, Klene M, Knox JE, Cross JB, Bakken V, Adamo C, Jaramillo J, Gomperts R, Stratmann RE, Yazyev O, Austin AJ, Cammi R, Pomelli C, Ochterski JW, Martin RL, Morokuma K, Zakrzewski VG, Voth GA, Salvador P, Dannenberg JJ, Dapprich S, Daniels AD, Farkas O, Foresman JB, Ortiz JV, Cioslowski J, Fox DJ (2009) Gaussian 09, Revision A.1. Gaussian, Inc, Wallingford CT
30. Kamtekar KT, Wang C, Bettington S, Batsanov AS, Perepichka IF, Bryce MR, Ahn JH, Rabinal M, Petty MC (2006) J Mater Chem 16: 3823
31. Prachumrak N, Pojanasopa S, Tarsang R, Namuangruk S, Jungsuttiwong S, Keawin T, Sudyoadsuk T, Promarak V (2014) New J Chem 38:3282
32. Collado D, Casado J, Gonzalez SR, Navarrete JTL, Suau R, Perez-Inestrosa E, Pappenfus TM, Raposo MMM (2011) Chem Eur J 17: 498
33. Qu JQ, Pschirer NG, Liu DJ, Stefan A, Schryver FCD, Mullen K (2004) Chem Eur J 10:528
34. Ohkita H, Benten H, Anada A, Noguchi H, Kido N, Ito S, Yamamoto M (2004) Phys Chem Chem Phys 6:3977